ELECTROMAGNETIC INTERACTION BETWEEN PERMANENT MAGNETS AND BULK Y-Ba-Cu-O SUPERCONDUCTORS

Ken Nagashima*, Tomohiko Murayama#, Tsuyoshi Otani*
and Masato Murakami*
* Superconductivity Research Laboratory, ISTEC
1-16-25, Shibaura, Minato-ku, Tokyo 105, Japan
now at Shikoku Electric Power Company
2-5 Marunouchi, Takamatsu-shi, Kagawa 760, Japan

ABSTRACT

We have measured the electromagnetic force (EMF)[1] between Nd-Fe-B magnets and bulk Y-Ba-Cu-O superconductors, by varying magnet configurations such as the number of poles, the thickness of magnets and back iron yokes, the number of subsectioned magnets and the shape of bulk superconductors and studied the effects of these variables on the EMF. The EMF is strongly dependent on the magnet configuration, and therefore for the design of magnetic bearings in a superconducting flywheel system, it is very important to optimize the arrangement of permanent magnets for achieving a large EMF.

INTRODUCTION

Stable levitation or suspension of a heavy object in midair can be realized using a combination of a strong permanent magnet and a bulk superconductor with high critical current density (J_c) [1]. Recent progress in the fabrication of good quality large Y-Ba-Cu-O bulk superconductors with high Jc made it possible to levitate a person at 5 cm gap[2], and the force density has already reached 1kg/cm^2 [3]. Several applications with levitation have been proposed and those are magnetic bearings, flywheels, and transport systems. The feasibility studies of these systems have already been performed worldwide [4]. In particular, a super conducting flywheel system for energy storage is attractive when superconducting magnetic bearings are installed,since the rotational loss of the bearing can be greatly reduced. For this reason, a number of superconducting flywheel systems have been constructed and subjected to field testing [5],[6]. Through these studies, it has been confirmed that rotational loss of the superconducting flywheel system can really be reduced to a very small value [7]. However, for practical applications it is also very important to increase the stored energy, which requires a large EMF.

It is known that the EMF between a superconductors and a magnet is given by

$$F = \int m \nabla H dv \qquad (1)$$

[1]Editors Note: The standard abbreviation for electromotive force is emf (all lower case letters). Hence, the nonstandard abbreviation for electromagnetic force, EMF, uses all upper case letters to distinguish it from electromotive force.

In one dimension, this equation is simplified as

$$F = m\frac{dH}{dx} \tag{2}$$

where m is the magnetic moment of a superconductor, and dH/dx is a field gradient produced by a magnet. A number of studies have been conducted for the electromagnetic interaction between a single magnet and a single superconductor [8],[9]. Numerical simulation has also been conducted and found to be in good agreement with the experimental results [10]. In most experiments, however, the relative position of a permanent magnet and a superconductor is symmetric with their central axes fixed on the same line.

In contrast to such a simple case, the configuration of magnets/superconductors for practical flywheel is more complicated and the position of bulk superconductors and permanent magnets is off-axis.

In the present study, we then prepared various flywheels, in which Nd-Fe-B magnets with different configurations are assembled in an aluminum plate, and measured the EMF between these flywheels and bulk Y-Ba-Cu-O superconductors as a function of the gap in order to deduce a generic trend in the EMF.

EXPERIMENTAL

Bulk Y-Ba-Cu-O superconductors with the cation ratio of Y: Ba: Cu = 1.8: 2.4: 3.4 were prepared with the top-seeded melt-growth (TSMG) method, the details of which are described elsewhere [11],[12]. In the TSMG process, prior to the melt-growth process, a $SmBa_2Cu_3O_y$ seed crystal is positioned at the center of the pellet so that the c-axis of the seed is aligned perpendicularly to the top surface. With this technique, a large single-grain Y-Ba-Cu-O bulk with the c-axis oriented parallel to the pellet surface can be fabricated.

In order to study the effect of the size and shape of superconductor on the EMF, we prepared two kinds of YBCO bulks: 4.5 cm in diameter and 2.0 cm in height; and 4 cm square and 2 cm in thickness. For EMF measurements, these superconductors are placed in a thermally insulating container, as schematically shown in Fig. 1. In this arrangement, the c-axis of Y-Ba-Cu-O bulks is directed parallel to the magnetic field of permanent magnet, whereby induced currents mainly flow within the a-b plane, that is a preferred orientation for the supercurrent flow.

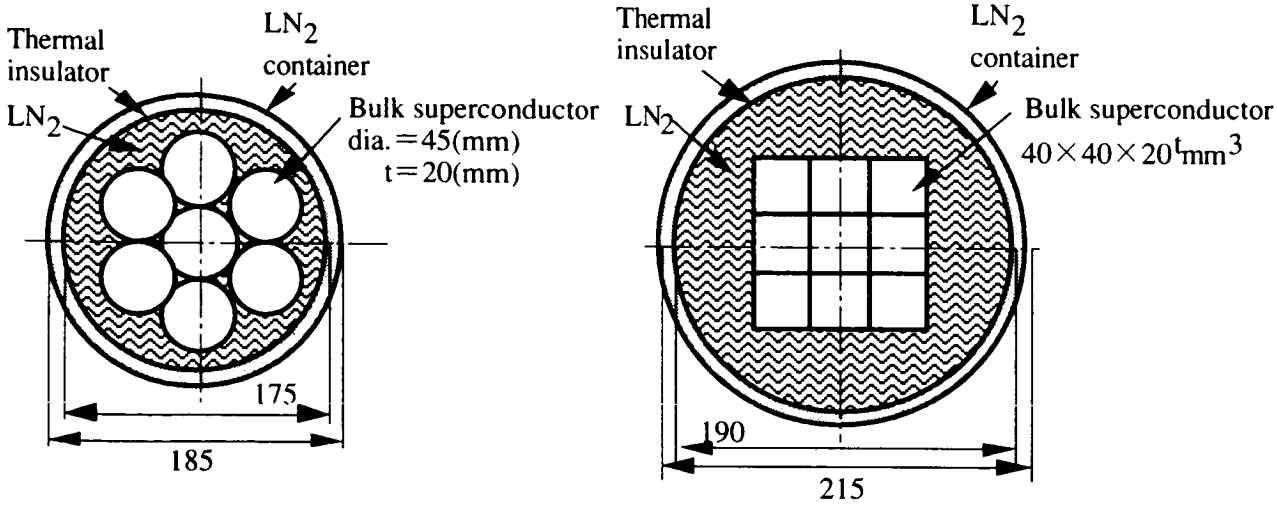

(a) Disk bulks (b) Rectangular bulks

Fig 1. Arrangements of superconductors.

Table 1. Specification of permanent magnets used in this study.

Magnet No.	Number of Poles	Thickness of Yoke	Thickness of Magnets	Weight of Magnets	Notes
No.1	1	0mm	10mm	1.15kg	
No.2	1	0mm	15mm	1.57kg	
No.3	1	0mm	34mm	3.27kg	
No.4	1	10mm	15mm	2.22kg	
No.6	1	8mm	15mm	1.71kg	2 subsectioned
No.7	1	8mm	15mm	1.78kg	3 subsectioned
No.8	2	8mm	10mm	1.58kg	
No.9	2	8mm	15mm	2.00kg	
No.11	2	8mm	34mm	3.57kg	
No.12	2	8mm	15mm	1.94kg	spacer 3 mmt
No.13	2	8mm	15mm	1.87kg	spacer 6 mmt
No.14	3	8mm	15mm	1.99kg	
No.15	4	8mm	15mm	1.98kg	

Flywheel (Permanent Magnets)

In order to study the effect of magnetic field distribution, we have prepared flywheel disks with various magnet configurations, as specified in Table 1 and also schematically presented in Fig 2. Permanent magnets used in the present experiment were Nd-Fe-B with B_r = 1.3 T.

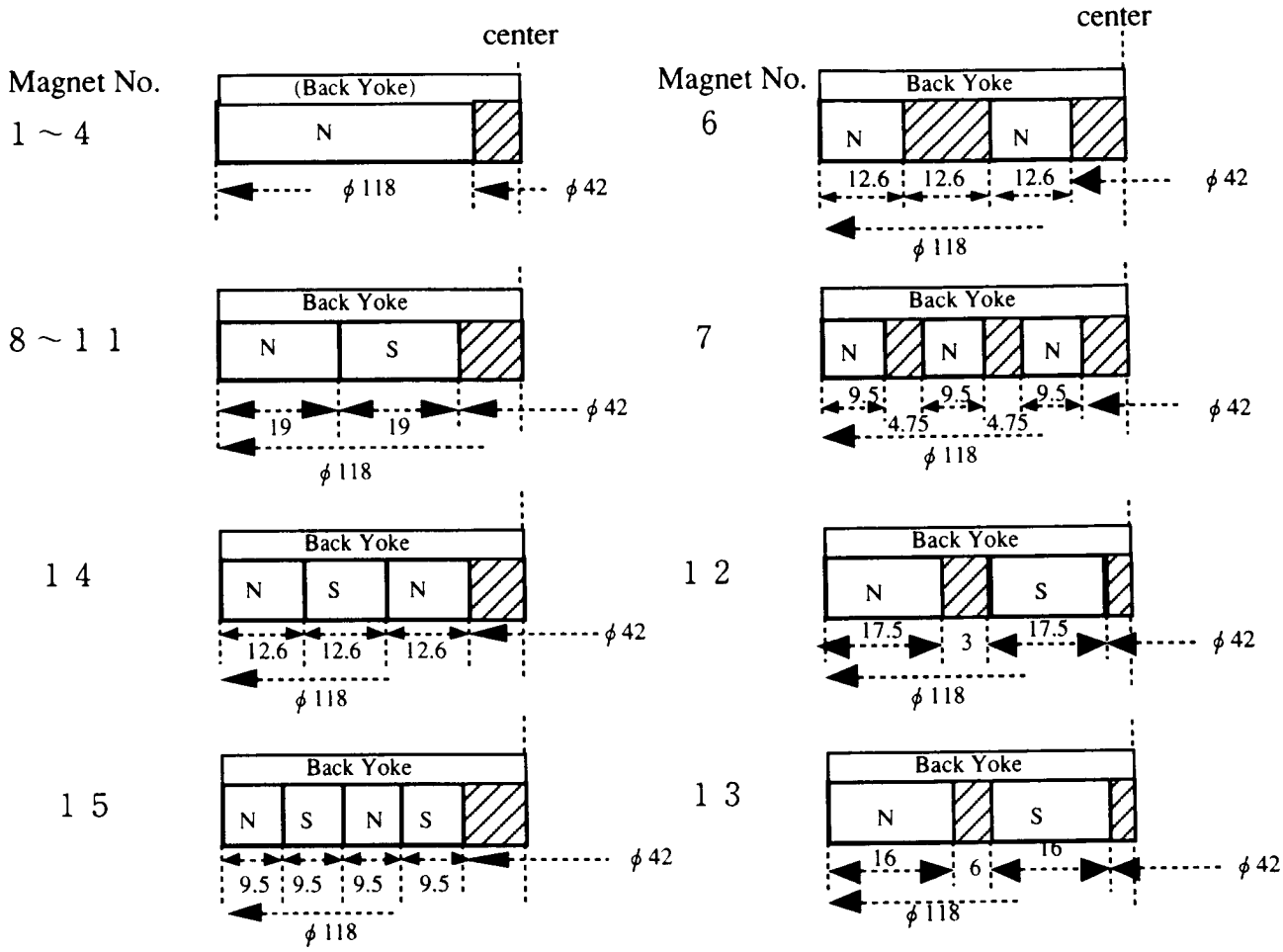

Fig 2. Configurations of permanent magnets.

Measurement of Repulsive Force

Figure 3 shows a schematic of the apparatus (Shimadzu Autograph AGS-100D) for the EMF measurements between the flywheel and bulk superconductors. Here, the flywheels are attached to a load cell and brought toward bulk superconductors which are arranged and glued to the thermal insulating container and cooled by liquid nitrogen, as already illustrated in Fig. 1.

EMF measurement procedure was as follows. Bulk superconductors are cooled in liquid nitrogen

in zero field while keeping the distance far enough to avoid the effect of the field generated from the magnet. Next the flywheel is moved to the position 50mm above the superconductors and then moved toward the superconductors for EMF measurements. The gap is automatically controlled by a computer and the EMF is continuously recorded as a function of the gap with a data acquisition system during both descending and ascending processes.

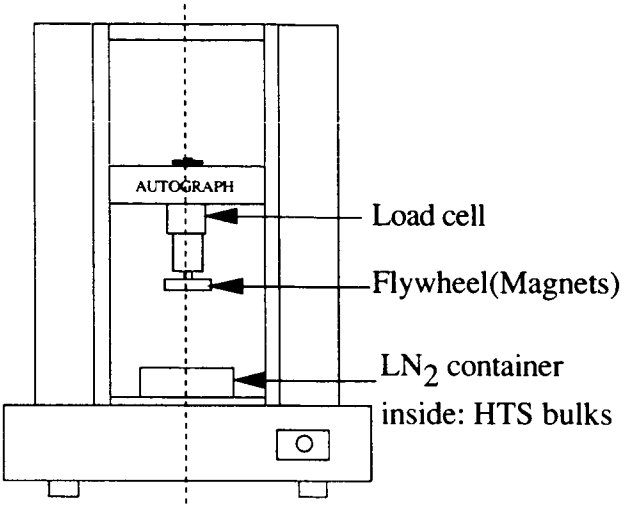

Fig 3. The schematic of the experimental setup.

RESULTS AND DISCUSSION

The Effects of Arrangement and Shape of Superconductors

Figure 4 shows the relationship between the force density and the magnet/superconductor gap for disk and rectangle bulks. Here we used three kinds of magnets with different thickness (No. 1, No.2 and No. 3). And the force density is the amount of repulsive force divided by the area of arranged bulk superconductors. It is clear from the figure that the force density curves for two different superconductors almost overlap, indicating that the shape of the superconductor has a very small effect on the EMF. We could not see any appreciable difference due to the shape of superconductors for almost all the magnets studied in the present study, which shows that the effect of the shape is negligible for the EMF.

The source of EMF is the interaction between the induced currents and magnetic field. Induced currents can flow within the pinned superconductor only at the surface layer. The penetration depth of induced (or shielding) currents is a function of J_c of the superconductor. In one dimension, the penetration depth (dx) is given by the following equation:

$$\frac{dB}{dx} = \mu_0 J_c \qquad (3)$$

where μ_0 is the permeability of vacuum, and dB is the external magnetic induction. The EMF is also given by the equation (2), in which m is the magnetization of a superconductor. Here it should be born in mind that the magnetization of the superconductor is obtained because the interior region is shielded by the induced currents. Figure 5 is a schematic illustration of the magnetization of the superconductor, in which dx is the penetration depth in the equation (3) and the internal field gradient (dB/dx) gives J_c. Y-Ba-Cu-O superconductors used in this experiment exhibit J_c of 30000 - 50000 A/cm^2 at 77 K and 0.1 - 0.5 T, which is the field strength used in this experiment. The penetration depth is thus in the order of 0.1 mm, which is much smaller than the dimension of the superconductors, showing that the most volume can be shielded by induced currents. Therefore, even if we change the shape of the superconductor, there will be no drastic change in the magnetization per unit volume, which is the reason that the shape of a superconductor has a small effect on the EMF.

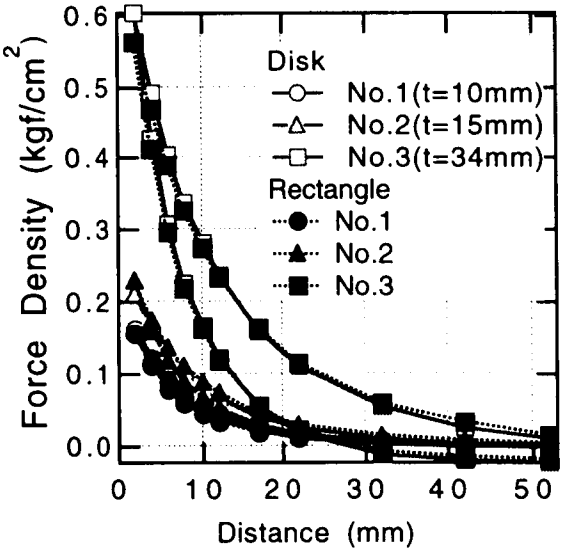

Fig 4. Relationship between the force density and the magnet/superconductor gap for disk and rectangle bulks.

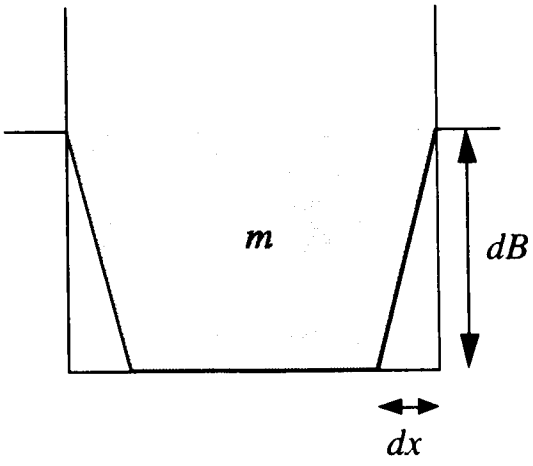

Fig 5. Schematic illustration of the magnetization of the superconductor.

Effect of Thickness of Single-pole Permanent Magnets

It is well known that as the thickness of permanent magnet is increased, the demagnetizing effect (or the geometrical effect) is reduced. Therefore the magnetic field at the surface of magnet pole

increases with increasing the thickness, as shown in Fig 6. Accordingly the repulsive force has the tendency to increase as the thickness of permanent magnet is increased (see Fig. 4). This shows that the EMF can simply be increased by increasing the thickness of the magnet. As an economical way to increase the effective thickness of the magnet, it is common to attach an iron yoke to the back of a magnet. Figure 7 shows the effect of the effective thickness on the EMF (magnets No.2 and No.4). It is clear that the EMF could also be increased simply by increasing the yoke thickness. However, it should also be born in mind that the weight of the levitated magnet increases with increasing magnet thickness. This suggests that we should take account of the EMF per unit volume rather than the EMF per unit area when the weight of the levitated magnet is important.

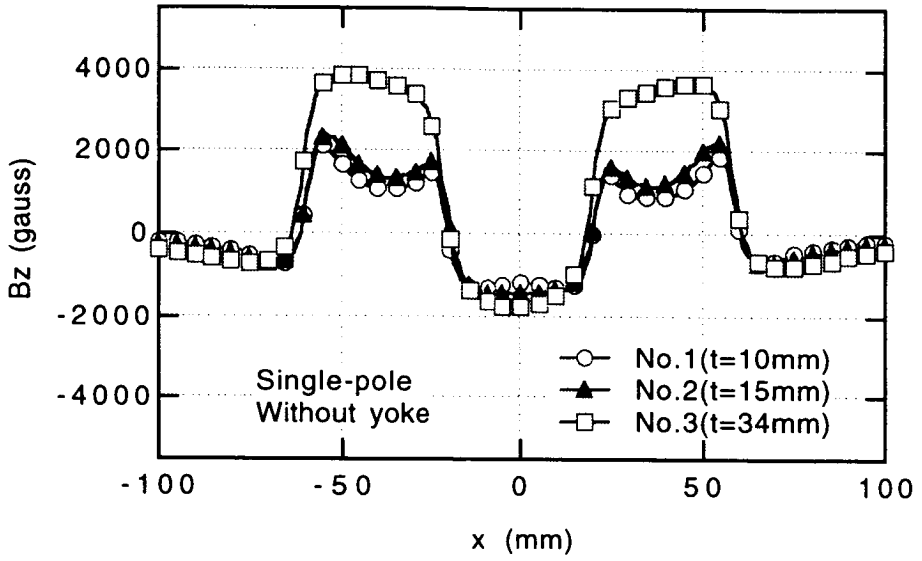

Fig 6. Magnetic field distribution at the surface of flywheel (Gap=2.8mm).

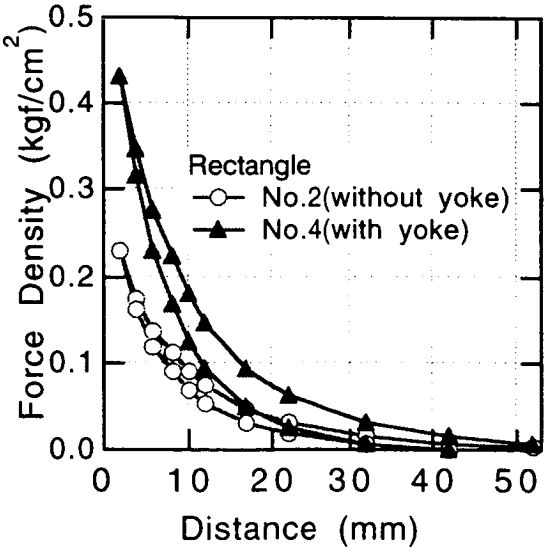

Fig 7. Force density vs. the magnet/superconductor gap.

Effect of Thickness of Double-pole Permanent Magnets

Figure 8 shows magnetic field distribution of double-pole magnets. For these magnets, an iron yoke with 8mm thickness was attached to increase the effective thickness. Like the case of a single-pole magnet, the peak magnetic field strength increases with increasing magnet thickness. Accordingly, the EMF increases with increasing magnet thickness as shown in Fig. 9, although the effect of magnet thickness was not so drastic compared with a single pole magnet. It is also notable that while the EMF is large for a single-pole magnet even at a relatively large gap, for a double-pole magnet the EMF is smaller in a large gap region but steeply increases with decreasing gap and surpasses the value of a single-magnet when the gap is below 5 mm. Such behavior can easily be understood in terms of the difference in the field distribution for single and double-pole magnets as shown in Fig. 10. For a double-pole magnet, the field and the field gradient are very strong only near the surface due to the fact that magnetic flux generated from one pole cannot diverge and must direct the pole with the opposite sign, and therefore the EMF is very strong in a small gap region and decays quickly with the gap. In contrast, for a single-pole magnet, since the magnetic flux spans a longer distance, the EMF does not decay with the gap like a double-pole magnet, instead the EMF near the surface is smaller. These results clearly show that for the design of a flywheel, the necessary gap for magnet/superconductor is important for optimization of the magnet arrangement in order to achieve a large EMF under operational conditions.

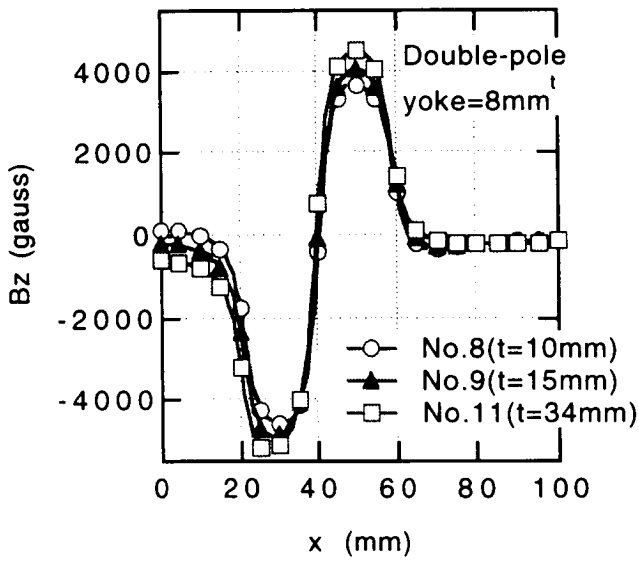

Fig 8. Magnetic field distribution(Gap=2.8mm).

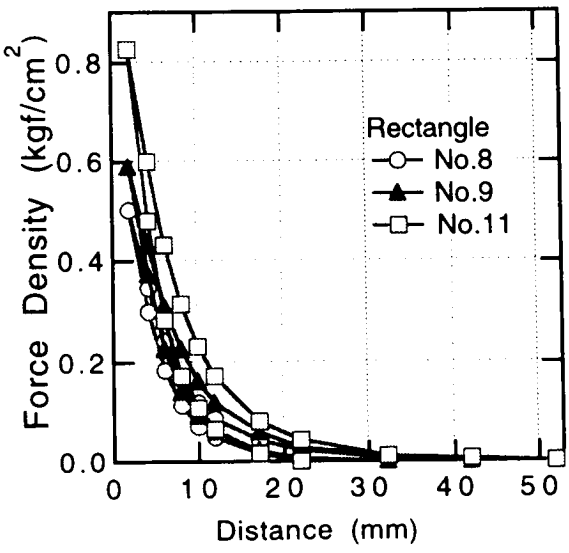

Fig 9. Force density vs. the magnet/bulks gap.

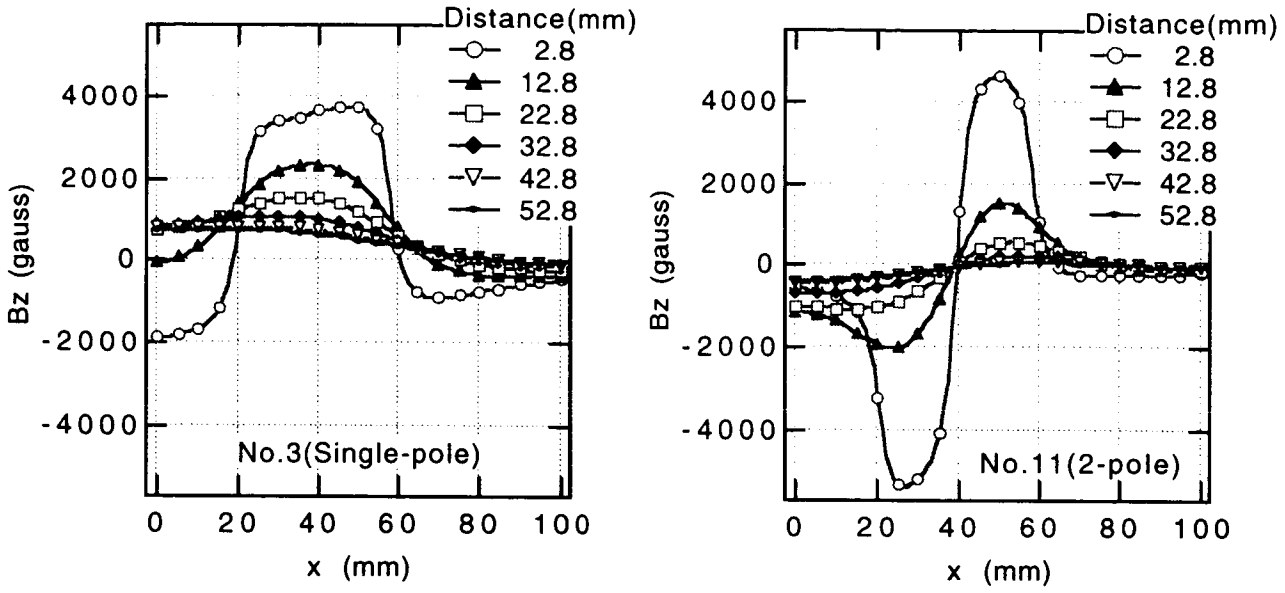

Fig 10. Gap dependence of magnetic field distribution.

The Effects of Number of Poles

Figure 11 shows the magnetic field distribution of the magnets with different pole numbers: magnets No.4, No9, No.14 and No.15. At the gap of 2.8 mm, the peak field strength is not a simple function of the number of poles. As discussed above, the field is localized for multi-pole magnets near the magnet surface, and the field distribution is strongly affected by the width of each pole and also the thickness of the magnet. Here, except for single-pole magnet, the effective thickness of multi-pole magnets is constant. When the number of poles is increased, the effective distance between two neighbor poles is reduced and the field will tend to be more localized near the surface. The fact that the peak field strength of a four-pole magnet (No. 15) is smaller than two- or three-pole magnets (No. 9 and No. 14) at 2.8 mm gap may indicate that the most field cannot span this gap for a four-pole magnet.

Figure 12 is a relationship between the force density and the gap for these magnets. In a large gap region, a single-pole magnet gives the highest force density, which can be understood by the fact that magnetic field can span a longer distance. In a small gap region, there are several interesting features. First, the force density of a four-pole magnet is the smallest. Second the largest force density is recorded for a double-pole magnet below 5 mm gap. These results show that a simple increase in the pole number is not effective in increasing the EMF. It is also interesting to note that the EMF strength near the magnet surface is the largest for a double-pole magnet and the smallest for a four-pole magnet, which contrasts with the idea of simple field localization, and indicates that magnetic flux density in free space may be small for multi-pole magnets, which should be taken into

account for the design of flywheels.

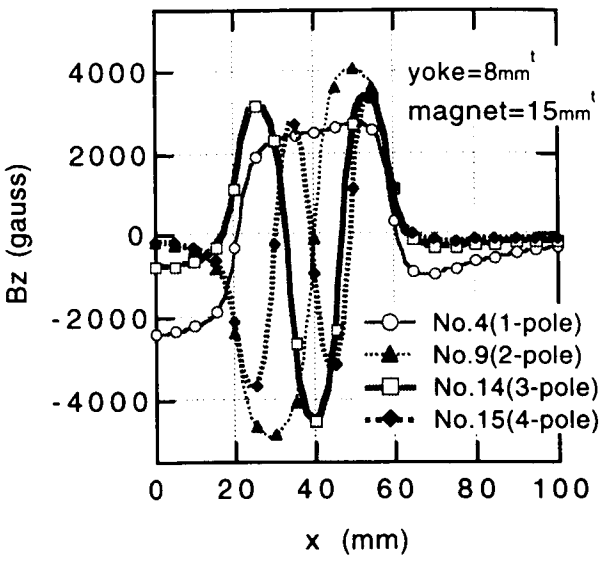

Fig11. Magnetic field distribution at the surface of flywheel (Gap=2.8mm).

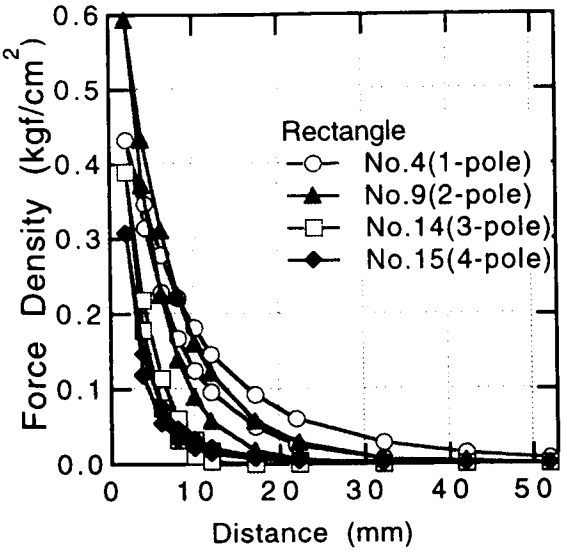

Fig12. Force density vs. the magnet/bulks gap.

The Stiffness of Flywheel

For the application of flywheel, the EMF along the radial direction or the stiffness is also important. In the present experiment, it was difficult to directly measure the stiffness, however, a general trend we found is that the levitation of the flywheel with multi-pole magnets is more stable than single-pole magnets, indicating that the stiffness is large for multiple-pole magnets.

According to equation (2), the EMF along radial direction (F_x) can be given by

$$F_x = \frac{m}{\mu_0}\frac{dB_z}{dx} \qquad (4)$$

and therefore, the distribution of dB_z/dx is one of the important parameters to evaluate the stiffness. Figure 13 shows the variation of dB_z/dx along a radial direction for single-pole (No.3) and a four-pole (No.15) magnet. As clearly be seen in the figure, the peak height is much higher for a four-pole magnet, indicating that the stiffness is higher. Thus an increase in the pole number is effective in enhancing the radial stability, although it was not so effective in increasing the EMF for levitation.

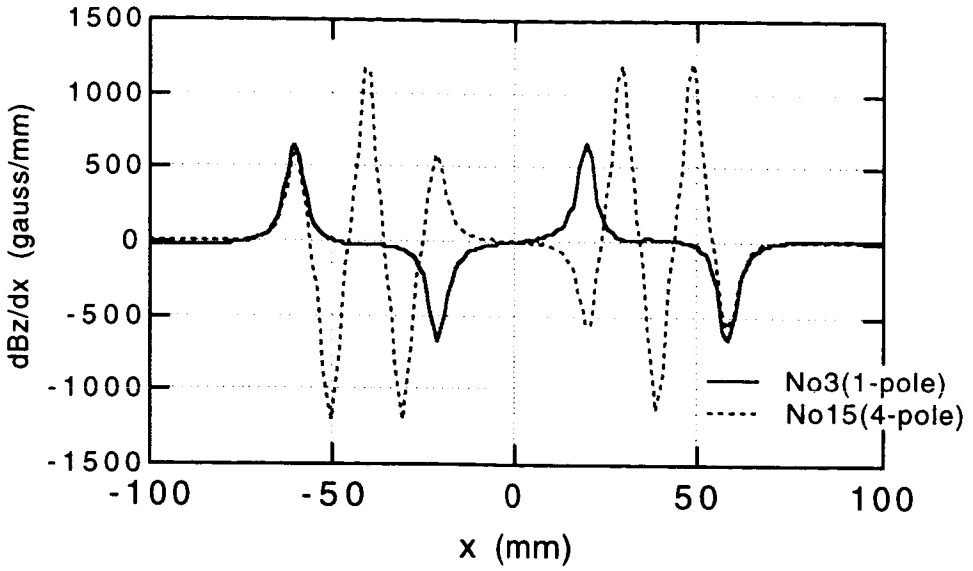

Fig 13 The dB_z/dx distribution of permanent magnets (Gap=2.8mm).

Effect of Subsectioned Magnets

The demagnetizing effect can also be reduced by increasing the effective magnet height, that is, to subsection the single-pole magnet part of magnet No.2 like the magnets No.6 and No.7, the configuration of which is already presented in Fig.2. The magnetic field strength at the surface will be increased by such treatment. Figure 14 shows the magnetic field distribution of these magnets at 2.8mm gap. Compared to a single-pole magnet, subsectioned magnets exhibit higher peak field, however, the peak field of the magnet subsectioned in three sectors is lower than that of two-subsectioned magnet. This can be understood by considering the fact that the total magnet volume, and therefore the total flux density is reduced by subsectioning the magnet, and this loss in the total flux density is responsible for a low magnetic field strength of three-subsectioned magnet.

Figure 15 shows the relationship between the force density and the gap for these magnets. Despite the increased field strength, an increase in the force density due to the subsection treatment is very small. The effect may become clear when the force density is normalized with the effective surface area of the subsectioned magnet. In conclusion, the subsectioning is not so effective in increasing the EMF. However, in manufacturing a flywheel for practical use, it is customary to insert a spacer between the magnets to support the mechanical strength of Nd-Fe-B magnets, since their strength is of order 8 kg/mm^2 and much smaller than that of engineering materials. In this context, the fact that the EMF was not reduced by inserting the spacer is favorable for the design of practical flywheel.

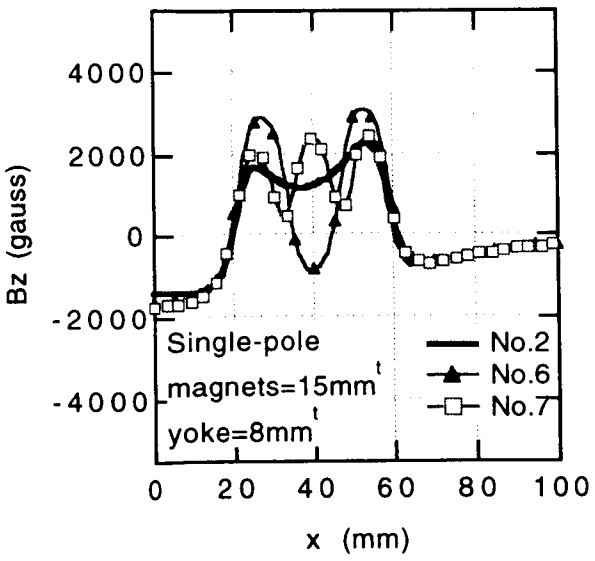

Fig14. Magnetic field distribution at the surface of flywheel (Gap=2.8mm).

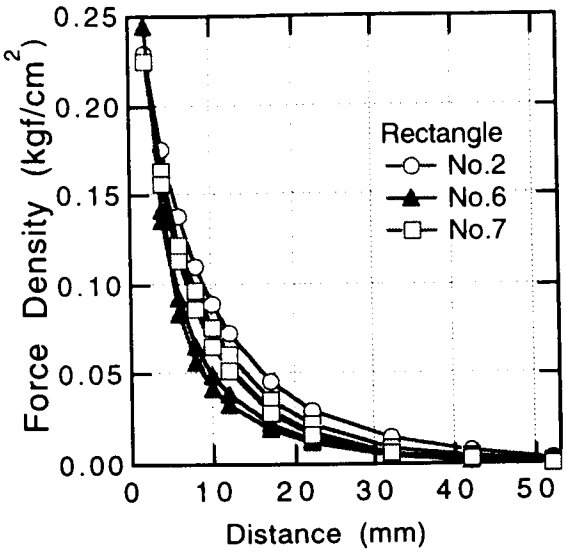

Fig15. Force density vs. the magnet/bulks gap.

Effects of a Spacer for Double-pole Magnet

We have also studied the effect of a spacer on the EMF of a double-pole magnet, and the configuration of the magnets (No. 12 and No. 13) is already presented in Fig. 2. Figure 16 shows the field distribution for magnets No. 9, No. 12, No. 13. It is clear that the field distribution is almost identical, showing that the effect of a spacer is very small. As a result, the effect of a spacer on the force density is also quite small for a double-pole magnet, as shown in Fig. 17. Such small effect of a spacer may be in part due to a relative small width ratio of the magnet to the spacer for the present experiment, and clear effect may be seen if the width of spacer is increased. The magnetic flux lines cannot be curved by a small angle, that is, the critical angle exists for the bending of magnetic flux, and therefore when the south and north poles are aligned with their axes parallel to each other like the case of the present study, magnetic flux near the S/N boundary cannot come out of the magnet, so that the contribution of the magnet near the boundary to the external field is negligibly small. In other words, the magnetic field will not be reduced even when we insert the spacer for the construction of practical flywheel.

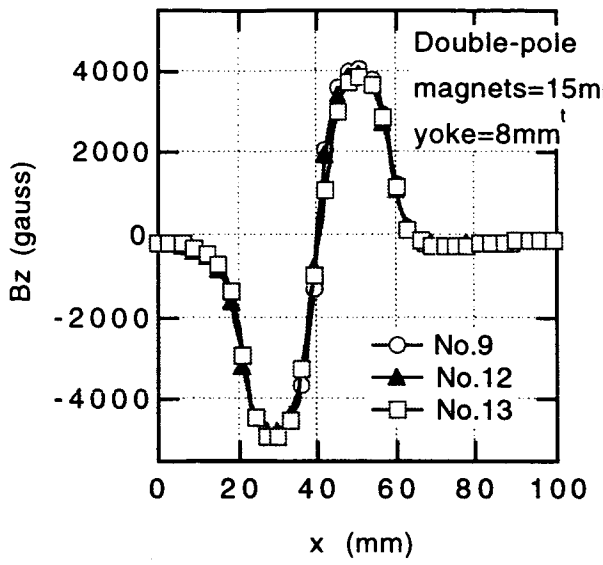

Fig16. Magnetic field distribution at the surface of flywheel (Gap=2.8mm).

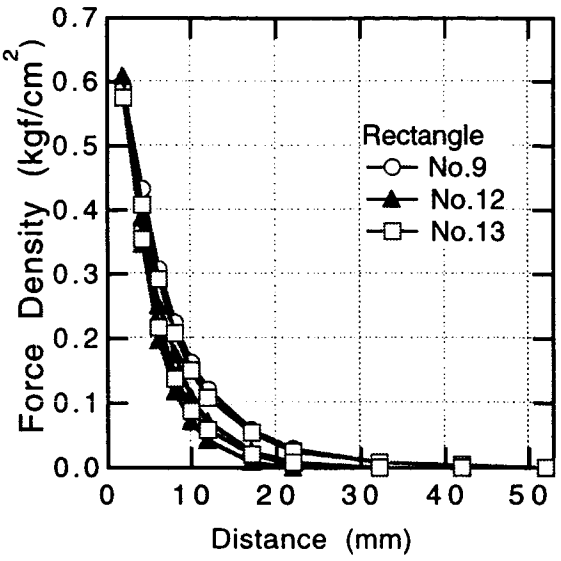

Fig17.Force density vs. the magnet/bulks gap.

SUMMARY

From the present experiments, several interesting features could be deduced as to the electromagnetic interaction between multiple magnets and multiple superconductors. First, the EMF was almost independent of the shape of the superconductors with high J_c. Second the EMF was strongly dependent on the magnet configuration, in that the field distribution was the most important factor to govern the EMF. For the design of the flywheel as well as other levitation systems, it is important to optimize the thickness, the width, the number of poles of magnet for achieving a large EMF. It should also be born in mind that the optimal magnet configuration is the function of the gap, at which the system is operated.

ACKNOWLEDGMENTS

The authors are grateful to Sumitomo Special Metals for the design of the flywheel magnets used in the present study. This work was supported by NEDO for R&D of Industrial Science and Technology Frontier Program.

REFERENCES

1. Murakami, Masato ed.: *Melt Processed High-Temperature Superconductors.* World

Scientific Publ. Co., Pte. Ltd., 1992.

2. Yoo, S.I.; Fujimoto, H.; Sakai, N.; Murakami, M.: Melt-processed LRE-Ba-Cu-O superconductors and prospects for their applications. *J. Alloys and Compounds,* vol. 250, 1997 pp. 439-448.
3. Kondoh, A.; Kagiya, S.; Takaichi, H.; Sakai, N.; Murakami, M.: YBaCuO with Large Magnetic Repulsive Force. *Advances in superconductivity 5*, Springer-Verlag Tokyo, 1993 pp. 1301-1304.
4. Nagaya, S.; Hirano, N.; Takenaka, M.; Minami, M.; Kawashima, H.: Fundemental Study on High Tc Superconducting Magnetic Bearings for Flywheel System. *IEEE Trans. Appl. Supercond.* vol. 5, No. 2, June 1995, pp. 643-649.
5. Bornemann, H. J.; Urban, C.; Boegler, P.; Ritter, T.; Zaitsev, O.; Weber, H.; Rietschel, H.: High speed superconducting flywheel system for energy storage. *Physica C* , vol. 235-240, 1994, pp. 3455-3456.
6. Bornemann, H. J.; Tonoli, A.; Ritter, T.; Urban, C.; Zaitsev, O.; Weber, K.; and Rietschel, H.: Engineering Prototype of a Superconducting Flywheel for Long Term Energy Storage. *IEEE Trans. Appl. Supercond.* vol. 5, No. 2, June 1995, pp. 618-621.
7. Hull, J. R.; Mulcahy, T. M.; Uherka, K. L.; Abboud R. G.: Low Rotational Drag In High-Temperature Superconducting Bearings. *IEEE Trans. Appl. Supercond.* vol. 5, No. 2, June 1995, pp. 626-629.
8. Hiebel, P.; Tixador, P.; Brunet, Y.; Chaud, X.; Beaugnon, E.; de Rango, P.; Ducloux, F.; Tournier, R.: Characterization of magnetically textured YBaCuO pellets and permanent magnet configurations for applications to magnetic bearings. *Physica C* , vol. 235-240, 1994, pp. 3449-3450.
9. Matsuura, K.; Homma, N.; Sawada, N.; Tsuchimoto, M.; Yamada, K.; Honma, T.: Observations of Suspension and Levitation Effects of Bulk HTSCs in microgravity Experiments. *Advances in superconductivity 7*, Springer-Verlag Tokyo, 1995 pp. 821-824.
10. Tsuchimoto, M.; Homma, N.; Matsuura, K.; and Matsuda, M.: Numerical Evaluation of Levitation Force of a Thin Film High Tc Superconductor. *Advances in superconductivity 9*, Springer-Verlag Tokyo, 1997 pp. 1389-1392.
11. Morita, M.; Sawamura, M.; Takebayashi, S.; Kimura, K.; Teshima, H.; Tanaka, M.; Miyamoto, K.; and Hashimoto, M.: *Physica C* , vol. 235-240, 1994, p. 209.
12. Morita, M.; Tanaka, M.; Takebayashi, S.; Kimura, K.; Miyamoto, K.; and Sawano, K.: *Jpn. J. Appl. Phys.*, vol. 30[5A], 1991, p. 813.